CERN Report CERN-2022-XXX

Tentative Parameter list for the International Muon Collider Collaboration

Authors: IMCC

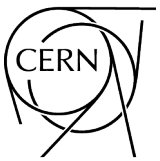

Tentative Parameter list for the International Muon Collider Collaboration (IMCC)

Author: IMCC

Abstract

This document comprises a tentative list of parameters for the IMCC together with assumptions made. The tentative parameter list is the first attempt of the IMCC to document a complete self-consistent muon collider, from the proton driver to the detector. Particular attention has been given to regions of the facility that are believed to hold greater technical uncertainty in their design.

Keywords

Collider, muon, accelerator physics, technology

Contents

1 Introduction and general considerations

This document contains the tentative parameters for the MuCol study. The parameters will be developed in several iterations, starting with this one, to finally reach consolidated parameters.

This collection of tentative parameters includes high-level goals, such as the target beam parameters at different key interfaces of the collider complex. It also contains many parameters that have been developed bottom-up by the teams that work on the different parts of the complex and different technologies. These parameters in part are already the fruit of the R&D of each team or they are goals that the team considers realistic goals based on their expertise and studies carried out so far. They allow to better judge the overall parameters. By adding important details they also allow identification of further development needs.

Currently very little optimisation has been performed. The planned further development of performance, cost and power consumption models will allow revision and optimisation of the parameters.

The current parameter set broadly assume a new site; in reality the facility would likely built at an existing laboratory. Significant reuse of existing infrastructure would be possible in this case. Studies to exploit this opportunity are ongoing and not yet included in the parameters.

1.1 Schedule Considerations

By the end of MuCol (March 2027) a planning for the further R&D and a path to the muon collider will be established. The current considerations are to develop a two-staged approach. The first stage could be at around 3 TeV centre-of-mass energy and the second at 10 TeV. The first stage is based on technology that we expect to be ready for production in about 15 years. The technology for the second stage has to be ready about 15 years later. At this moment it is considered that the first stage can be based on the use of high-temperature superconducting (HTS) solenoids in the muon production and cooling. The collider ring would use $\mathrm{Nb_3Sn}$-based dipoles. For the second stage HTS and hybrid dipole designs can be used.

The plan takes into account the availability of human resources. A large part of the human resources will be committed during the seven years of construction and the first five years of commissioning and operation of the collider. Only limited R&D on key technologies can be undertaken during this time. During the next three years human resources would become increasingly available to develop the technical design of the second stage. Consequently the construction can start for the second stage about 15 years after the first stage.

The operation of the first stage will continue during the construction of the second stage. At the end of the construction a period of probably about two years is required to connect the last RCS of the first stage with that of the second stage. Also some improvements in the complex might be implemented. These considerations indicate that the first stage should operate for about 13 years. One or two long shutdowns may be required during this time. At this moment we assume about two years for this. This number has to be refined. Compared to LHC the collider is more complex but smaller. At the beginning the collider will not achieve full luminosity but have to be ramped up. The first two to three years are expected to provide as much integrated luminosity as one year at full luminosity. The total integrated luminosity over 13 years would thus be equivalent to nine to ten years of full luminosity operation. Achievement of the physics goals requires about five years of full luminosity operation at the expected achievable luminosity.

The plan is consistent with considerations of potential physics needs in different regions:

– CERN's current strategy is to show the feasibility of FCC-ee and to implement the FCC programme. The muon collider is considered as a plan B in the case that this strategy needs to be adjusted. This requires the operation to start several years after the end of the HL-LHC programme. At this moment this means well before 2050.
– In the US high-energy physics community, strong interest in the muon collider exists including an ambition to realise it in the US on a realistic timescale, which is also well before 2050.

Therefore, it is important to establish that a first stage of the muon collider can indeed be considered with start of construction in around 15 years. The second stage will reuse almost the full complex of the first stage with the exception of the 4.5 km-long collider ring.

1.2 Muon Colliders

Muon colliders can in principle reach the highest lepton collision energies with the required luminosity. Detailed cost and power consumption calculations have not been performed but simple scalings indicate that the facility will be affordable. This allows unprecedented exploration in direct searches of new heavy states and high-precision tests of Standard Model phenomena. The required luminosity increase, with the square of the energy, can in principle be provided with a constant beam current, i.e. with an only linear increase in the beam power with energy.

The full physics potential at high energies remains to be quantified but first explorations are encouraging. For example, the number of produced Higgs bosons will allow measurement of Higgs couplings to fermions and bosons with an unprecedented precision. Moreover, a collider with a centre-of-mass energy in the range of $\sqrt{s} \simeq 10$ TeV or above and with a luminosity of the order of 10^{35} cm^{-2} s^{-1} will have a very high double and triple Higgs-boson production rate, which will allow direct measurement of the trilinear and quadrilinear self-coupling parameters, enabling precise determination of the Higgs boson potential. An important concern is the impact of the high background level induced by muon beam decay products. Detailed studies are being undertaken, including potential mitigation methods. Recent results demonstrated that the measurement of $\mu^+\mu^- \to H\nu\overline{\nu} \to b\bar{b}\nu\overline{\nu}$ process is feasible in this harsh environment, with a precision on $\sigma(\nu\nu H)\cdot\text{BR}(H \to b\bar{b})$ at the level of less than 1% at $\sqrt{s} = 3$ TeV, competitive to other proposed machines.

In addition to the technical challenges, two main limitations exist for the energy reach of the muon collider. The first is given by the cost and site requirements. Therefore an optimisation for cost and footprint is an important consideration during the design phase. The second limitation is given by the ability to achieve the required luminosity with an affordable power consumption and cost. The current baseline is to aim for $L \simeq (\frac{\sqrt{s}}{10\text{TeV}})^2 \times 2 \times 10^{35}$ cm^{-2} s^{-1}. The muon collider could be implemented in energy stages to limit the cost and risk of each stage, while still providing excellent physics. The choice of stages will also depend on future findings of the HL-LHC and other relevant colliders. First considerations yielded the following tentative conclusions that will be reviewed as the work progresses:

– The design effort should focus on a high energy stage at 10 TeV with a luminosity of 2×10^{35} cm^{-2} s^{-1}. This will demonstrate feasibility of a high energy stage matching approximately the physics reach of the FCC-hh.

- A first stage will be explored at 3 TeV with a luminosity of 1.8×10^{34} cm^{-2} s^{-1}. This matches the maximum energy of CLIC and is a good point to compare the merits of the approaches.
- A dedicated design effort for a muon collider at lower energies (below 3 TeV) is feasible, but requires dedicated additional studies. Currently no studies are foreseen but this will have to be reviewed as the progress and choices of other projects become clearer.

Successful implementation of a muon collider is based on a wide range of cutting edge technologies. In particular, key technologies are:

- High field, robust and cost-effective superconducting magnets for the muon production, cooling, acceleration and collision. High-temperature superconductors would be an ideal option.
- High-gradient and robust normal-conducting RF to minimise muon losses during capture and cooling.
- Fast ramping normal-conducting, super-ferric or superconducting magnets that can be used in a rapid cycling synchrotron to accelerate the muons supported by pulsed power converters with millisecond level ramping times.
- Efficient, high-gradient superconducting RF to minimise power consumption and muon losses during acceleration.
- Efficient cryogenics systems to minimise the power consumption of the superconducting components and minimise the impact of beam losses.
- Robust materials for muon cooling and also collimation and machine protection.
- Advanced detector concepts and technologies to deal with the background induced by the muon beams.
- Other accelerator technologies including high-performance, compact vacuum systems to minimise magnet aperture and cost as well as fast, robust, high-resolution instrumentation.

Laboratories in Europe and world-wide have important expertise in these areas and could further develop these technologies to enable a muon collider and push its performance reach. The formation of a collaboration to initiate and coordinate a development programme appears indispensable. In the first phase of the programme, the development of the baseline, this effort would largely draw on the experience while in later stages it will focus more on prototyping. At least one test facility will be required to develop the muon collider concept to address the most critical challenges. The production of a high quality muon beam will be key and most likely the lion share of this effort. The collaboration will have to develop the experimental beam programme and its implementation drawing on the expertise of the contributing laboratories.

The reuse of existing infrastructure can have a significant impact on the cost and risk of a muon collider. Hence, the potential to use and modify the existing proton installations and related infrastructure should be investigated as well as the reuse of existing buildings, tunnels and services. The muon source requires a high proton beam current, and one can consider upgrading the existing proton infrastructure to meet the requirements. Other equipment could be used for the new complex, e.g. existing cooling plants could potentially be used for the accelerator and collider rings. The main reuse of tunnels is for the accelerator and for the collider ring. The latter should be as small as possible to maximise luminosity. The former will be longer and has less stringent requirements on the length. It is therefore expected to

profit more from existing tunnels. An important consideration for the tunnels is the neutrino flux. It can come from the arcs or more important from the straight insertions. Civil engineering studies should identify the locations of highest neutrino flux. It may be possible to improve the situation by acquiring the surface sites corresponding to the highest flux. A detailed study is being performed of mitigation by a special optics design. One can envisage to bend the beam in the vertical plane using alternating sets of dipoles to produce a wave-like orbit.

1.3 Structure of the Document

The overall parameters are listed followed by parameters for each subsystem, starting with the proton driver, passing through to the front end, the muon beam cooling, acceleration and then the collider ring. Details of underlying technologies are given in subsequent sections. Finally, the Machine-Detector interface and Detector parameters are described. It should be noted that some systems, such as the initial muon acceleration, are still based on old designs from the MAP study. Also the matching of the parameters at the interfaces has not been completed in all cases as it requires trade-offs across the boundaries; this will be a prime goal for the next iteration.

2 Target Parameters and Luminosity Considerations

The top-level parameters for the facility are shown in Table 2.1 and 2.2. A two stage approach is considered where the first stage could be constructed on a timescale consistent with the end of HL-LHC operation and construction of the second stage would follow.

Table 2.1: Tentative target parameters for a muon collider at different energies based on the MAP design. These values are only to give a first indication. It should be noted that the longitudinal charge profile is assumed to extend to a radius of 2 standard deviations. Beamstrahlung (BS) is calculated for the first collision. Energy and photon numbers will decrease in proportion to the muon beam charge. The total loss is approximated using this rough scaling. The target luminosity allows to reach the integrated luminosity target in nine to ten years of operation at $1\text{–}1.1 \times 10^7$s per year. Estimated luminosities and beamstrahlung are based on the target parameters and beam-beam simulations with a new version of GUINEA-PIG.

Parameter	Symbol	unit	Stage 1	Stage 2
Centre-of-mass energy	E_{cm}	TeV	3	10
Target luminosity (5 years)	$\mathcal{L}_{target,5}$	$10^{34}\text{cm}^{-2}\text{s}^{-1}$	1.8	20
Target Luminosity (10 years)	$\mathcal{L}_{target,10}$	$10^{34}\text{cm}^{-2}\text{s}^{-1}$	1	10
Estimated luminosity	$\mathcal{L}_{estimated}$	$10^{34}\text{cm}^{-2}\text{s}^{-1}$	2.1	21
Collider circumference	C_{coll}	km	4.5	10
Collider arc peak field	B_{arc}	T	11	16
Luminosity lifetime	N_{turn}	turns	1039	1558
Muons/bunch	N	10^{12}	2.2	1.8
Repetition rate	f_r	Hz	5	5
Beam power	P_{coll}	MW	5.3	14.4
RMS longitudinal emittance	$\varepsilon_{\parallel}$	eVs	0.025	0.025
Transverse emittance	$\varepsilon_{\perp}$	µm	25	25
IP bunch length	σ_z	mm	5	1.5
IP betafunction	β	mm	5	1.5
IP beam size	σ	µm	3	0.9
Protons on target/bunch	N_p	10^{14}	5	5
Protons energy on target	E_p	GeV	5	5
BS photons	$N_{BS,0}$	per muon	0.075	0.2
BS photon energy	$E_{BS,0}$	MeV	0.016	1.6
BS loss/lifetime (2 IP)	$E_{BS,tot}$	GeV	0.002	1.0

Table 2.2: Tentative target beam parameters along the acceleration chain. A 10 % emittance growth budget has been foreseen in the transverse and longitudinal planes, both for 3 and 10 TeV. This assumes that the technology and tuning procedures will have been improved between the two stages. The interface between final cooling and acceleration is chosen at about 150 MeV kinetic energy, which implies that some acceleration is performed at the end of the final cooling stage. This choice allows to optimise the final energy of the final cooling with no strong impact on the acceleration chain.

Parameter	Symbol	Unit	Final Cooling	Inj. at 3 TeV	Inj. at 10 TeV
Beam total energy	E_{beam}	GeV	0.255	1500	5000
Muons/bunch	N_b	10^{12}	4	2.2	1.8
Longitudinal emittance	$\varepsilon_{\parallel}$	eVs	0.0225	0.025	0.025
RMS bunch length	σ_z	mm	375	5	1.5
RMS rel. momentum spread	σ_P/P	%	9	0.1	0.1
Transverse norm. emittance	$\varepsilon_{\perp}$	µm	22.5	25	25
Aver. grad. 0.2–1500GeV	G_{avg}	MV/m	—	2.4	
Aver. grad. 1.5–5TeV	G_{avg}	MV/m	—		1.1

3 Subsystem Parameters

3.1 Proton Driver

The parameters are tentative and based on previous studies such as the MAP and the Design for the Neutrino Factory at CERN. The proton driver is composed of a linac followed by two rings, an accumulator and a compressor, working both at fixed energy. The accumulators generate the bunch intensity and time structure, while the compressor reduces the bunch length according to the need of the subsequent muon capture. The parameters will be split in two blocks, the linac and the compressor which correspond to the main two tasks in the work package. For the high power linac (Table3.1) the tentative parameters are based on the the SPL design, assuming that the machine can be used for other experiments in addition to supporting the proton complex of the Muon Collider. The chopping scheme and minimum needed pulse length and charge will come eventually from the needs of the compressor and will be defined later in the project.

Table 3.1: Tentative Parameters for the H^- Linac.

	Linac		
Parameters	**Symbol**	**Unit**	**Value**
Final energy	E_{Linac}	GeV	5.0
Repetition rate	-	Hz	$\geq$5
Max. pulse length	-	ms	2.0
Max. pulse current	I_{Linac}	mA	40.0
Norm. rms emittance	ε_{Linac}	mm.mrad	2.5
Power	P	MW	2.0 (4.0*)
RF frequency	f_{RF}	MHz	352 and 704

* Possible future upgrade. Higher powers will be included in the study once a baseline solution is available.

If the need for beam energies above 5 GeV arises we assume that an accumulator similar to the J-PARC RCS can be used (with the needed scaling of energy and intensity) in order complete the acceleration and accumulation process before compression. The compressor ring (see Table 3.2) includes the main parameters range we will use to start investigating a possible solution. There are two options that will be studied, one using a beam with the final linac energy of 5 GeV and a second option with double the beam energy. The number of compressed bunches (and thus the single bunch charge in the compressor) is still a variable parameter since we cannot guarantee that a single pulse with the full charge can be store in a ring without causing major issues with respect to space charge and instabilities. For the compressing scheme a RF rotation will be employed. Optimisation of that system is ongoing and will determine transverse and longitudinal dynamics.

Table 3.2: Tentative parameters for the compressor.

Parameters	**Symbol**	**Unit**	**Option 1**	**Option 2**
Energy	E_{Ring}	GeV	5	10
Circumference	C	m	between 300 to 900	
Protons on target	n_p	-	5×10^{14}	2.5×10^{14}
Final rms bunch length	σ_z	ns	2	
Geo. rms. emittance	$\varepsilon_{x,y}$	π mm mrad	> 5	
Number of turns for phase rotation	N_{rot}	-	50	

3.2 Front End

The front end comprises the pion production target, beam cleaning chicane and proton absorber, and muon buncher and phase rotator that creates the initial bunch structure.

The overall parameters for the beam incident on the target are given in Table 3.3. The estimated outgoing beam parameters are listed in Table 3.4

Table 3.3: Baseline and range of beam parameters from the proton driver considered in the studies of the Carbon target systems.

Proton driver beam parameters				
Parameter	**Symbol**	**Unit**	**Baseline**	**Range**
Beam power	P	MW	2	1.5 - 3.0
Beam energy	E_{target}	GeV	5	2 - 10
Pulse frequency	-	Hz	5	5 - 50
Pulse intensity	n_p	10^{14} protons	5	3.7 - 7.5
Bunches per pulse	-	Number	1	1
Pulse length	σ_z	ns	2	1 - 2
Beam size	σ_x	mm	5	1 - 15
Impinging angle	-	degree	0.0	0.0 - 10

Table 3.4: Estimated outgoing beam.

Parameter	Symbol	Unit	Value
Number of Microbunches	n_b		21
Microbunch longitudinal emittance [mm]	ε_L	mm	46
Transverse emittance [mm]	$\varepsilon_\perp$	µm	17 000
μ^+ yield per GeV per proton on target	η^+	GeV^{-1} per proton	0.24
μ^- yield per GeV per proton on target	η^-	GeV^{-1} per proton	0.18

3.3 Cooling

The cooling system takes muons leaving the front end and reduces the beam phase space volume, resulting in increased luminosity. The two principle subsystems are a rectilinear cooling system and a final cooling system. The performance of the cooling system is summarised here. The simulated performance assumes approximately 40 % losses in the charge separation, initial rectilinear, bunch merge, and reacceleration after final cooling. The overall system performance parameters are listed in Table 3.5.

Table 3.5: Beam parameters entering and leaving the cooling system. The target emittances are listed. They are 10 % more demanding than the nominal emittances in the RCS and collider, allowing for some emittance growth at some point in the acceleration chain.

	$N_{bunches}$	Actual $\varepsilon_\perp$ [mm]	Target $\varepsilon_\perp$ [mm]	Actual ε_L [mm]	Target ε_L [mm]	Central p_z [MeV/c]	Transmission [%]
Entering	21	17.0	–	46.0	–	200	–
Leaving	1	0.052	0.0225	105	64	232	4.5

3.4 Updated Rectilinear Cooling

An updated rectilinear cooling system has been developed comprised of 10 "B-type" stages, denoted S1 through S10 that yields improved performance and has been designed using 352 MHz RF and harmonics. The performance is summarised in Table 3.6, improving on previous designs.

Table 3.6: Performance for the updated cooling system. A-stage and bunch merge performance is estimated based on previous studies. Charge separation parameters are target parameters as no design currently exists.

Stage	Transverse emittance $\varepsilon_\perp$ [mm]	Long. emittance ε_L [mm]	6D emittance ε_{6D} [mm^3]	Cumulative transmission [%]
initial	17.0	46.0	13300	100
Charge separation	17.0	46.0	13300	90
A-stages	1.48	2.35	260	46.8
Bunch merge	5.13	9.91	260	36.5
S1	2.85	8.74	71.13	31.3
S2	1.97	6.08	23.79	28.5
S3	1.42	3.43	7.21	25.1
S4	1.09	2.53	3.12	23.2
S5	0.72	2.24	1.22	20.6
S6	0.49	2.14	0.56	19.0
S7	0.35	2.16	0.27	18.5
S8	0.24	2.23	0.13	14.1
S9	0.19	1.81	0.067	11.1
S10	0.14	1.69	0.034	8.6

3.5 Updated Final Cooling

An updated final cooling system has been designed with performance listed in Table 3.7. A simplified longitudinal model is assumed at the end of each cooling cell. The system does not yet match target parameters. Inputs from the updated rectilinear cooling system have not been integrated. Optimisation continues.

Table 3.7: Beam parameters at the end of each cooling cell assuming a simplified longitudinal manipulation. Target numbers are listed for the section of acceleration required at the end of the system – no design exists.

Cell	LH length [m]	Transverse emittance $\varepsilon_\perp$ [mm]	Long. emittance ε_L [mm]	Energy spread σ_E [MeV]	Bunch length σ_z [mm]	Beam mom. $P_{z,end}$ [MeV/c]	Cumulative trans. N [%]
1	0.85	0.232	2.6	1.45	194	135	98
2	0.6	0.189	4.8	2.4	216	135	97
3	0.58	0.168	7	2.9	253	128	95
4	0.66	0.144	12.3	3.6	364	120	93
5	0.5	0.125	22	4.4	520	118	92
6	0.56	0.118	31	5.0	620	104	91
7	0.25	0.101	41	4.4	970	92	87
8	0.15	0.089	49	4.1	1240	95	85
9	0.15	0.078	60	3.3	1900	78	80
10	0.123	0.065	73	3.1	2400	75	76
11	0.103	0.052	105	3.5	3200	75	73
Accel.	0	0.052	105	3.5	3200	232	38

3.6 Low-Energy Acceleration

The low-energy acceleration section consists of a single-pass, superconducting linac with 325 MHz RF cavities, accelerating muons to 1.25 GeV, that captures the muon phase-space after the final cooling channel. The linac was designed to have a large acceptance suitable for a relatively high emittance beam for neutrino production as a potential pre-stage for the muon collider. The large acceptance of the linac requires large apertures and tight focusing. This, combined with moderate beam energies, favors solenoid rather than quadrupole focusing for the entire linac. Two different sections were designed, comprising two different cryomodules. Table 3.8 contains same of the key parameters of the linac.

The linac is followed by a 4.5-pass, recirculating linear accelerator (RLA) in a 'dogbone' configuration that accelerates from 1.25 to 5 GeV. In this scheme, acceleration beyond 1.25 GeV continues using a more compact and efficient 650 MHz SRF structure. Then, for final part of the low-energy acceleration (from 5 GeV to 62.5 GeV) the above RLA is followed by an additional 5-pass 'dogbone' configuration RLA. In this scheme, acceleration continues using a 1.3 GHz SRF structure. Table 3.9 contains parameter details for both RLA1 and RLA2

Table 3.8: Parameters describing the single-pass linac that follows the final cooling section. Energies are total energies.

	CryoModule 1	CryoModule 2
Initial energy [GeV]	0.255	
Final energy [GeV]		1.25
No. SRF cavities	22	30
RF length [m]	1	2
Frequency [MHz]	325	325
RF gradient [MV/m]	20	20
Passes	1	1

Table 3.9: Parameters describing the multi-pass 'dogbone' recirculating linac. Energies are total energies.

	RLA1	RLA2
Initial energy [GeV]	1.25	5
Final energy [GeV]	5	62.5
No. SRF cavities	38	490
RF length [m]	2	4
Frequency [MHz]	650	650
RF gradient [MV/m]	25	25
Passes	4.5	5

3.7 High-Energy Acceleration

We summarize the parameters of the high-energy acceleration chain. Four rapid cycling synchrotrons are listed, values for the fourth are draft parameters. We assume fixed survival rate of 90% per accelerator.

Table 3.10: Summary table of the acceleration chain. Emittances listed in the table are 10 % higher than those leaving the cooling system, to allow for emittance growth during the acceleration. The muon loss rate in RCS4 is a factor 2 smaller than the goal, potentially allowing to halve the RF voltage.

Parameter	**Symbol**	**Unit**	**RCS1**	**RCS2**	**RCS3**	**RCS4**
Hybrid RCS	-	-	No	Yes	Yes	Yes
Repetition rate	f_{rep}	Hz	5	5	5	5
Circumference	C	m	5990	5990	10700	35000
Injection energy	E_{inj}	GeV/u	63	314	750	1500
Ejection energy	E_{ej}	GeV/u	314	750	1500	5000
Energy ratio	$E_{\text{ej}}/E_{\text{inj}}$	-	4.98	2.39	2.00	3.33
Assumed survival rate	$N_{\text{ej}}/N_{\text{inj}}$	-	0.9	0.9	0.9	0.9
Acceleration time	τ_{acc}	ms	0.343	1.097	2.37	6.37
Revolution period	T_{rev}	µs	20	20	36	117
Number of turns	n_{turn}	-	17	55	66	55
Required energy gain per turn	ΔE	GeV	14.8	7.9	11.4	63.6
Average accel. gradient	G_{avg}	MV/m	2.44	1.33	1.06	1.83
Number of bunches/species	-	-	1	1	1	1
Bunch population at injection	N_{inj}	1×10^{12}	2.7	2.4	2.2	2.0
Bunch population at ejection	N_{ej}	1×10^{12}	2.4	2.2	2.0	1.8
Vertical norm. emittance	$\epsilon_{\text{v,n}}$	mm	25	25	25	25
Horiz. norm. emittance	$\epsilon_{\text{h,n}}$	mm	25	25	25	25
Long. norm. emittance $\sigma_E \times \sigma_t$	$\epsilon_{\text{z,n}}$	eVs	0.025	0.025	0.025	0.025
Tot. straight section length	L_{str}	m	2335	2336	3976	10367
Total NC dipole length	L_{NC}	m	3655	2539	4366	20376
Total SC dipole length	L_{SC}	m	0	1115	2358	4257
Max. NC dipole field	B_{NC}	T	1.80	1.80	1.80	1.80
Max. SC dipole field	B_{SC}	T	-	10	10	16
Ramp rate	$\dot{B}$	T/s	4200	3282	1519	565
Main RF frequency	f_{RF}	MHz	1300	1300	1300	1300
Max RF voltage	V_{RF}	GV	20.9	11.2	16.1	90

3.8 Collider

The present work concentrates on the design of a 10 TeV center of mass collider. The aim is to maximize the luminosity to the two possible experiments. The basic assumptions are extrapolations from lower energy starting with a relative rms momentum spread of $\sigma_\delta = 1 \cdot 10^{-3}$. Together with the longitudinal emittance, this fixes the rms bunch length $\sigma_z = 1.65\,\text{mm}$ and the $\beta^* = 1.65\,\text{mm}$ to the same value (such that the hour glass luminosity reduction factor $f_{hg} = 0.758$ starts to become significant). Maximization of the luminosity requires to choose the shortest possible circumference C compatible with feasibility of the magnets (average bending field assumed to be $\bar{B} \approx 10.48\,\text{T}$ leading to $C \approx 10\,\text{km}$). Note that extrapolation of parameters to higher energies lead to very large chromatic effects further increasing with energy.

The main parameters are described in Table 3.11. Magnet radial build and cryogenic requirements are described in Tables 3.12 and 3.13

Table 3.11: Tentative parameters of a 10 TeV center of mass muon collider studied at present.

Parameter	Symbol	Unit	Value
Center of mass energy		TeV	10
Beam energy	E	TeV	5
Relativistic Lorentz factor	γ		47 322
Circumference	C	m	$\approx$ 10 000
Dist. of last magnet to IP	L^*	m	6
Repetition rate	f_r	Hz	5
Bunch intensity (one bunch per beam)	N_μ		$1.8 \cdot 10^{12}$
Injected beam power per beam	P_B	MW	7.2
Normalized transverse rms emittance	$\varepsilon_\perp$	µm	25
Longitudinal norm. rms emittance $\sigma_E\sigma_t$	$\varepsilon_\parallel$	eVs	0.025
Relative rms momentum spread	$\sigma_\delta = \sigma_p/p$		$1 \cdot 10^{-3}$
RMS bunch length in space	σ_z	mm	1.5
RMS bunch length in time domain	σ_τ	ns	0.005
Twiss betatron function at the IP	β^*	mm	1.5
Transverse rms beam size at the IP	$\sigma^*_\perp$	µm	0.9

Table 3.12: Tentative 1D radial build of the collider arcs, defining the inner aperture of coils (10 TeV). All units are mm.

	Thickness	Outer radius
Beam aperture	23.49	23.49
Coating (copper)	0.01	23.5
Radiation absorber (tungsten alloy)	40	63.5
Shielding support and thermal insulation	11	74.5
Cold bore	3	77.5
Insulation (Kapton)	0.5	78
Clearance to coils	1	79

Table 3.13: Fundamental design requirements for the cryogenic design of superconducting magnets for the collider ring.

		Comments
Overall electrical power consumption of cryogenic system of the collider magnets	$\leq$ 2.5 kW/m	Based on 25 MW assumed for cryogenic operation of the collider ring (8% of 300 MW estimated electrical power from the 2021 Snowmass Report
Temperature level of the absorber	$\geq$ 250 K	Assuming 500 W/m heat loads at absorber level (tungsten shielding).
Heat load deposited on the coil	$\leq$ 10 W/m	Heat intercept between coil and absorber is compulsory to fulfil this requirement.
Temperature level of the coil/cold mass	$\geq$ 4.5 K	Efforts must be made to substantially reduce the overall amount of cooling fluid

3.9 RF

The RF parameters which can be considered are listed below.

Table 3.14: Possible RF frequencies and gradients to be used by beam dynamics studies.

Proton driver				
Linac				
RF frequencies	MHz	352	704	
Muon cooling complex				
6D-cooling channels				
RF frequencies	MHz	352	704	1056
Maximum accelerating field in cavity (conservative)	MV/m	22	30	30
Maximum accelerating field in cavity (optimistic)	MV/m	35	50	50
Acceleration complex				
Linacs				
RF frequencies	MHz	352	704	1056
Maximum accelerating field in cavity (conservative)	MV/m	20	25	30
Maximum accelerating field in cavity (optimistic)	MV/m	30	38	45
RCSs				
RF frequency	MHz		704	1056, 1300
Maximum accelerating field in cavity (conservative)	MV/m		25	30
Maximum accelerating field in cavity (optimistic)	MV/m		38	45

In the other sub-systems of the muon cooling complex, for example in the capture, bunch merge and final cooling, many different RF frequencies are necessary. It is recommended to keep these RF frequencies as high as reasonable possible from the beam dynamics point of view, since the size of the achievable gradient scales approximately as $\sqrt{(f_{RF})}$.

3.10 Magnets

Table 3.15: Summary of magnet development targets. RCS Normal Conducting (NC) magnets are ramped but all other magnets are Steady State (SS).

Complex	Magnet	Aperture [mm]	Length [m]	Field [T]	Ramp-rate [T/s]	Temperature [K]
Target, decay and capture	Solenoid	1200	19	20	SS	20
6D cooling	Solenoid	90–1500	0.08–0.5	4–15	SS	4.2–20
Final cooling	Solenoid	50	0.5	>40	SS	4.2
Rapid cycling synchrotrons	NC Dipole	30×100	5	$\pm$ 1.8	4200	300
	SC Dipole	30×100	1.5	10	SS	4.2–20
Collider ring	Dipole	160–100	4–6	11–16	SS	4.2–20

The main magnet performance targets and target ranges (i.e. not yet a specification) for the most challenging magnets of the MuC are listed in Table 3.15. The parameters identify a feasible magnet performance range that can be achieved on the time scale of construction of a muon collider. Though these targets are bound to adapt as the muon collider study proceeds, they already provide a good basis to feedback on beam optics and accelerator performance, and to identify outstanding issues to be addressed by future work and dedicated R&D. The work has a strong focus on HTS. A trivial reason is the required field reach, in particular for the target and final cooling solenoids that would not be possible otherwise. But, just as important, this is also because of considerations of efficient cryogenic operation and helium inventory. Operation at temperatures in helium gas in the range of 10 to 20 K can offer a coefficient of performance up to a factor four higher than a cryoplant producing liquid helium at 4.2 K. Higher energy efficiency is mandatory to cope with the energy deposition generated by the muon decay and ensuing cascades, which applies throughout the muon collider complex.

Given the relatively young state of HTS magnet technology, we do not exclude that the range identified in Table 3.15, and that it could be extended further. This will however require at the minimum a proof-of-principle, especially in the case of the dipole and quadrupole magnets needed by the collider. Such advances may take place on a timeline longer than envisaged for the first stage of realization of the muon collider, and could be considered for later upgrades.

3.11 Power Converters

In the design and management of power converters, the acceleration of muon beams presents the most significant challenge. The current strategy employs a hybrid system of both normal and superconducting dipoles and quadrupoles magnets to steer the beams. Among these, the normal conducting magnets are pivotal for pulsing, making their associated power converters especially critical for development. Key parameters for sizing the power converters for the RCS are delineated in Table 3.16. Owing to the substantial peak power and voltage requirements, it is envisioned that the power converters will be distributed throughout the accelerator across numerous sectors. Each sector functions as an electrically distinct unit, which must be precisely controlled.

Table 3.16: Important dimensioning values for the power converters of the RCS.

			RCS1	**RCS2**	**RCS3**	**RCS4**
Total length	l_{mag}	km	3.65	2.54	4.37	20.38
Max flux density	B_{max}	T	1.8	1.8	1.8	1.8
Air gap width	w_g	mm	100	100	100	100
Air gap height	h_g	mm	30	30	30	30
Magnets peak energy	E_{mag}	MJ	21.2	14.7	25.3	118.2
B ramping time	T_{ramp}	ms	0.35	1.1	2.37	6.37
Repetition times	T_{rep}	ms	200	200	200	200
Magnets inductance	L_{mag}	uH/m	6.3	6.3	6.3	6.3
Magnets Resistance	R_{mag}	uΩ/m	69.3	69.3	69.3	69.3
Power converter peak power	P_{pk}	GW	121	54	43	74
Power converter peak current	I_{peak}	kA	43	43	43	43
Power converter total output voltage	V_{outpk}	MV	2.8	1.27	1.03	1.88

Given the considerable peak power levels required, a resonance-based approach will be adopted for the design of the power converters. The primary components of a resonance circuit are the capacitors and inductors, which establish the resonance. The design objective for the power converters is to limit the installed resonant capacitative and inductive energy, ensuring that the desired resonance is effectively generated in the resistive magnets.

3.12 Impedance Models

The transverse impedance model for the first Rapid Cycling Synchrotron (RCS) of the high energy acceleration chain assumes that $O(700)$ Low-Loss type of TESLA superconducting RF cavities are used. The number of cavities follows from the requirement on the energy gain per turn to keep a beam survival rate of $90\,\%$.

Transverse beam dynamics simulations for the RCS 1 were performed to investigate the effect of the RF system with a single high intensity bunch. The main parameters are summarised in Table 3.17.

Table 3.17: Summarised parameter list used for transverse collective effects simulations in the RCS 1.

Parameter	**Symbol**	**Unit**	**Value**
Circumference	C	m	5990
Injection energy	E_{inj}	GeV $c_0{}^{-1}$	63
Energy increase per turn	ΔE_{turn}	GeV	14.8
RF frequency	f_{RF}	MHz	1300
Total RF voltage	V_{RF}	GV	20.9
1σ bunch length	σ_z	mm	5.7
Transverse normalized emittance	ϵ_x/ϵ_y	µm rad	25/25
Average Twiss beta horizontal/vertical	β_x/β_y	m	50/50
Chromaticity	Q'_x/Q'_y		0/0
Detuning from octupoles horizontal/vertical		m^{-1}	0/0
Bunch intensity at injection	N_{inj}	muons per bunch	2.6×10^{12}

For the $10\,\mathrm{TeV}$ collider, impedance and transverse coherent beam stability studies were performed to determine the minimum chamber radius achievable. If a tungsten chamber with a $10\,\mu\mathrm{m}$ copper coating is used, with a 50-turn transverse damper gain, the minimum chamber radius required is $13\,\mathrm{mm}$, smaller than the $23.49\,\mathrm{mm}$ currently assumed for radiation shielding studies.

Table 3.18: Summarised impedance parameters for the $10\,\mathrm{TeV}$ collider

Parameter	**Symbol**	**Unit**	**Value**
Chamber geometry			circular
Chamber length	L	m	10000
Copper coating thickness		µm	10
Copper resistivity at 300 K	$\rho_{Cu,300K}$	$\mathrm{n}\Omega\,\mathrm{m}$	17.9
Tungsten resistivity at 300 K	$\rho_{W,300K}$	$\mathrm{n}\Omega\,\mathrm{m}$	54.4
Minimum chamber radius required (50-turn damper)	r_{min}	mm	13

Table 3.19: Summarised machine parameters for the 10 TeV collider impedance studies

Parameter	**Symbol**	**Unit**	**Value**
Circumference	C	metre	10 000
Beam energy	E	TeV	5
Bunch intensity at injection	N_b	muons per bunch	1.8×10^{12}
1σ bunch length	σ_z	mm	1.5
Transverse normalized emittance	$\epsilon_{x,y}$	μmrad	25
Momentum compaction factor	α_p		-2.0×10^{-6}
Synchrotron tune	Q_s		2.33×10^{-3}
Average Twiss beta	β_x/β_y	m	85/51
Chromaticity	Q'_x/Q'_y		0/0

3.13 Radiation

This section describes the decay-induced radiation load to collider ring magnets in the arcs (see Table 3.20), as well as the neutrino-induced dose distributions in soil for mono-directional muon beams (see Tables 3.21 and 3.22). The latter serve as dose kernels for computing the dose at the surface based on the collider optics and placement. The operational assumptions for the facility are documented in 3.23.

Table 3.20: Power load and radiation damage in collider ring arc magnets (10 TeV) as a function of the radial tungsten absorber thickness (derived with FLUKA). The power penetrating the shielding does not include neutrinos, since they are not relevant for the radiation load to the machine; the percentage values are given with respect to the power carried by decay electrons and positrons. The results include the contribution of both counter-rotating beams.

Absorber thickness [mm]	**20**	**30**	**40**
Beam aperture [mm]	23.5	23.5	23.5
Outer shielding radius [mm]	43.5	53.5	63.5
Inner coil aperture [mm]	59	69	79
Absolute power penetrating tungsten absorber [W/m]	19.1	8.2	4.1
Fractional power pentrating tungsten absorber [%]	3.8	1.6	0.8
Peak power density in coils [mW/cm^3]	6.5	2.1	0.7
Peak dose in Kapton insulation (5 years) [MGy]	56	18	7
Peak dose in coils (5 years) [MGy]	45	15	5
Peak DPA in coils (5 years) [DPA]	8×10^{-5}	6×10^{-5}	5×10^{-5}

Table 3.21: Effective dose kernel parameters of neutrino-induced radiation in soil at different baseline distances from the muon decay, for a muon beam energy of 1.5 TeV. The peak dose per muon decay and the lateral width of the dose profile (σ) have been derived from Gaussian fits of the FLUKA results.

	μ^-		μ^+	
Distance [km]	**Peak eff. dose [pSv/decay]**	**σ [m]**	**Peak eff. dose [pSv/decay]**	**σ [m]**
5	2.09×10^{-7}	0.17	2.19×10^{-7}	0.16
10	6.57×10^{-8}	0.32	6.56×10^{-8}	0.32
15	3.28×10^{-8}	0.47	3.34×10^{-8}	0.46
20	1.98×10^{-8}	0.60	1.99×10^{-8}	0.60
40	5.42×10^{-9}	1.17	5.49×10^{-9}	1.17
60	2.53×10^{-9}	1.71	2.51×10^{-9}	1.71
80	1.44×10^{-9}	2.29	1.42×10^{-9}	2.29
100	9.20×10^{-10}	2.85	9.21×10^{-10}	2.84

Table 3.22: Effective dose kernel parameters of neutrino-induced radiation in soil at different baseline distances from the muon decay, for a muon beam energy of 5 TeV. The peak dose per muon decay and the lateral width of the dose profile (σ) have been derived from Gaussian fits of the FLUKA results.

	μ^-		μ^+	
Distance [km]	**Peak eff. dose [pSv/decay]**	**σ [m]**	**Peak eff. dose [pSv/decay]**	**σ [m]**
5	1.57×10^{-5}	0.05	1.63×10^{-5}	0.05
10	4.86×10^{-6}	0.10	5.38×10^{-6}	0.10
15	2.54×10^{-6}	0.15	2.70×10^{-6}	0.14
20	1.56×10^{-6}	0.19	1.55×10^{-5}	0.20
40	4.80×10^{-7}	0.37	4.62×10^{-6}	0.38
60	2.33×10^{-7}	0.54	2.22×10^{-6}	0.55
80	1.38×10^{-7}	0.71	1.31×10^{-7}	0.73
100	9.16×10^{-8}	0.87	8.63×10^{-8}	0.90

Table 3.23: Parameters for radiation studies (collider ring). The number of decays consider the contribution of both beams.

	3 TeV	**10 TeV**
Particle energy [TeV]	1.5	5
Bunches/beam	1	1
Muons per bunch	2.2×10^{12}	1.8×10^{12}
Circumference [km]	4.5	10
Muon decay rate per unit length [$m^{-1}s^{-1}$]	4.9×10^9	1.8×10^9
Power ($e^{\pm}$) kW/meter	0.411	0.505
Operational years	5	5
Operational time per year (average)	1.2×10^7 s (=139 days)	1.2×10^7 s (=139 days)
Total decays per unit length (all years) [m^{-1}]	2.93×10^{17}	1.08×10^{17}

3.14 Machine-Detector Interface

This section describes the geometrical features of the shielding (nozzle) in the interaction region, which is essential for reducing the beam-induced background in the detector. The nozzle geometry defines the inner detector envelope (see Table 3.24) and the beam aperture near the interaction point (see Table 3.25). The section also quantifies the expected flux of secondary background particles due to muon decay, as well as the ionizing dose and displacement damage in different detector components (see Table 3.26). The particle flux and radiation damage estimates may still change in the future, depending on the final shielding and interaction region layout.

Table 3.24: Coordinates defining the outer surface of the MAP-like nozzle used in the background studies (azimuthal symmetry around the z-axis). The first point corresponds to the nozzle tip.

z [cm]	r [cm]
6	1
100	17.6
600	60

Table 3.25: Coordinates defining the inner aperture of the MAP-like nozzle used in the background studies (azimuthal symmetry around the z-axis). The first point corresponds to the nozzle tip.

z [cm]	r [cm]
6	1
15	0.6
100	0.3
600	2.3

Table 3.26: Maximum values of the ionizing dose and the 1 MeV neutron-equivalent fluence (Si) in a CLIC-like detector. All values are per year of operation (10 TeV) and include only the contribution of muon decay.

	Dose [kGy]	1 MeV neutron-equivalent fluence (Si) [10^{14} n/cm^2]
Vertex detector	200	3
Inner tracker	10	10
ECAL	2	1

3.15 Detectors

The main geometry parameters that describe the first detector concept at $\sqrt{s} = 3TeV$ are summarised in Table 3.27.

Table 3.27: Summary detector geometry. The distance from the last magnet to the interaction point is L^*=6m.

Barrel detector		
	R_{in} [cm]	R_{out} [cm]
Vertex tracker	3.1	10.2
Inner tracker	12.7	55.4
Outer tracker	81.9	148.6
ECAL	150.0	170.2
HCAL	174.0	333.0
Solenoid	348.3	429.0
Yoke	446.1	645.0

4 Appendix

In this appendix we describe the unit conversion between different commonly used longitudinal emittance definitions. We also describe the formulas for the calculation of the acceleration parameters of the high-energy acceleration chain.

4.1 Longitudinal Emittance - Unit conversion

When comparing literature, the longitudinal emittance of a particle bunch is usually given in different units. Also within the Muon Collider Collaboration, different units are used, with [mm], [eV-s] and [MeV-m] being the most common ones. To compare values in these different units, their conversion factors are determined as follows [1].

Between [MeV-m] and [eV-s]

The conversion factor between [MeV-m] and [eV-s] is c, the speed of light in vacuum. An emittance in units of [MeV-m] is converted to [eV-s] by dividing the value by c:

$$[\text{MeV-m}] \cdot \frac{1}{c} = [\text{eV-s}] \ . \tag{4.1}$$

As an example, the envisaged emittance of the muon collider of 7.5 MeV-m corresponds to 0.025 eV-s.

Between [mm] and [eV-s]

Papers from the MAP studies usually give longitudinal emittances in [mm]. Two definitions are used [2],

$$\epsilon_{\mathrm{L}} = \sigma_z \sigma_{\Delta p} / (m_\mu c) \ . \tag{4.2}$$

and

$$\varepsilon_{\mathrm{L}} = \sigma_t \sigma_E c / (m_\mu) \ . \tag{4.3}$$

The latter definition is more common, and especially is used for ionisation cooling studies by the analysis code ECALC9f. In this paper, the eq. 4.3 is used. The conversion factor from [eV-s] to [mm] is $m_\mu / c = 2839.35 \text{ mm eV}^{-1} \text{ s}^{-1}$.

4.2 The Survival Rate as a Function of Kinetic Energy

The survival rate of relativistic muons with an initial population of N_0 and a population of N after a certain time t is given as

$$\frac{N(t)}{N_0} = \exp\left(-\frac{t}{\gamma \tau_\mu}\right) \ , \tag{4.4}$$

where a constant γ is assumed. However, during acceleration, the kinetic energy of the muons and thus γ increases over time. For an acceleration time τ_{acc}, the survival rate is therefore calculated as

$$\frac{N(\tau_{acc})}{N_0} = \exp\left(-\frac{1}{\tau_\mu} \int_0^{\tau_{acc}} \frac{dt}{\gamma(t)}\right) \ . \tag{4.5}$$

Assuming a linear acceleration from injection energy E_{inj} with $\gamma_{inj} = \frac{E_{inj}}{m_\mu c^2} + 1$ to ejection energy E_{ej} and γ_{ej}, one can write the time-dependent Lorentz factor as

$$\gamma(t) = \gamma_{inj} + \frac{t}{\tau_{acc}}(\gamma_{ej} - \gamma_{inj}) \,. \tag{4.6}$$

The integral in Eq. 4.5 becomes

$$\begin{aligned} \int_0^{\tau_{acc}} \frac{dt}{\gamma(t)} &= \int_0^{\tau_{acc}} \frac{1}{\gamma_{inj} + \frac{t}{\tau_{acc}}(\gamma_{ej} - \gamma_{inj})} \\ &= \frac{\tau_{acc}}{\gamma_{ej} - \gamma_{inj}} \ln\left(\gamma_{inj} + \frac{t}{\tau_{acc}}(\gamma_{ej} - \gamma_{inj})\right)\Big|_0^{\tau_{acc}} \\ &= \frac{\tau_{acc}}{\gamma_{ej} - \gamma_{inj}} \ln\left(\frac{\gamma_{ej}}{\gamma_{inj}}\right). \end{aligned} \tag{4.7}$$

The survival rate is therefore

$$\frac{N(\tau_{acc})}{N_0} = \exp\left(-\frac{1}{\tau_\mu}\frac{\tau_{acc}}{\gamma_{ej} - \gamma_{inj}} \ln\left(\frac{\gamma_{ej}}{\gamma_{inj}}\right)\right) = \left(\frac{\gamma_{ej}}{\gamma_{inj}}\right)^{-\frac{1}{\tau_\mu}\frac{\tau_{acc}}{\gamma_{ej}-\gamma_{inj}}} . \tag{4.8}$$

The term only depends on the energy ratio and energy difference of the muons. For a fixed survival rate $\frac{N_{ej}}{N_{inj}}$ and fixed injection and ejection energies, i.e., fixed γ_{inj} and γ_{ej}, the acceleration time can be written as

$$\tau_{acc} = -\tau_\mu(\gamma_{ej} - \gamma_{inj}) \ln\left(\frac{N_{ej}}{N_{inj}}\right) / \ln\left(\frac{\gamma_{ej}}{\gamma_{inj}}\right) . \tag{4.9}$$

The number of turns in the machine for large particle energies, i.e. $\beta \approx 1$, is therefore:

$$\#\text{turns} = \frac{\tau_{acc}}{\tau_{rev}} = \frac{\tau_{acc} \cdot c}{2\pi R} . \tag{4.10}$$

4.3 Required Accelerating Gradient

We calculate the required accelerating gradient G_{acc} for a certain survival rate by rearranging Eq. 4.9:

$$\frac{\gamma_{ej} - \gamma_{inj}}{\tau_{acc}} = -\frac{1}{\tau_\mu} \ln\left(\frac{E_{ej}}{E_{inj}}\right) / \ln\left(\frac{N_{ej}}{N_{inj}}\right) , \tag{4.11}$$

while using that for large kinetic energies ($\gamma \gg 1$) one can approximate $\frac{\gamma_{ej}}{\gamma_{inj}} \approx \frac{E_{ej}}{E_{inj}}$. Inserting the definition of the Lorentz factor gives

$$\frac{E_{ej} - E_{inj}}{m_\mu c^2 \tau_{acc}} = G_{acc}\frac{c}{m_\mu c^2} = -\frac{1}{\tau_\mu} \ln\left(\frac{E_{ej}}{E_{inj}}\right) / \ln\left(\frac{N_{ej}}{N_{inj}}\right) , \tag{4.12}$$

or

$$G_{acc} = -\frac{1}{\tau_\mu} m_\mu c \ln\left(\frac{E_{ej}}{E_{inj}}\right) / \ln\left(\frac{N_{ej}}{N_{inj}}\right) , \tag{4.13}$$

where the mass (and energy) is given in units of eV. For a certain required survival rate, the minimum required acceleration gradient therefore only depends on the energy ratio E_{ej}/E_{inj} of the accelerator.

References

[1] F. Batsch, Unit conversion for longitudinal emittances (https://cernbox.cern.ch/index.php/s/lvooRxgtE8pZQ4j).

[2] A. Bogacz, *Muon Acceleration - Linac and RLA*, https://indico.cern.ch/event/973753/contributions/4100198/attachments/2143992/3613246/Linac%20and%20RLA.pdf, 2020